RSC Advances

ROYAL SOCIETY OF CHEMISTRY

www.rsc.org/advances

The First Study of Surface Modified Silica Nanoparticles in Pressure-decreasing Application

Caili Dai, Shilu Wang, Yuyang Li, Mingwei Gao, Yifei Liu, Yongpeng Sun, Mingwei Zhao*

School of Petroleum Engineering, State Key Laboratory of Heavy Oil Processing, China University of Petroleum (East China), Qingdao, Shandong, 266580, P. R. China

* Mingwei Zhao Email: zhaomingwei@upc.edu.cn

Tel: +86-532-86981183 Fax: +86-532-86981161

Abstract

In this study, hydrophobic silica nanoparticles were prepared by the surface modification of silica nanoparticles using dimethyldichlorosilane. Fourier transform infrared spectroscopy, thermogravimetric analysis, and X-ray photoelectron spectroscopy were employed for the characterization of the raw silica nanoparticles and modified silica nanoparticles. The results showed that methyl groups are successfully grafted on the surface of silica nanoparticles. The titration method was employed to quantitatively determine the surface hydroxyl number of silica nanoparticles, the result demonstrated that the surface hydroxyl number of silica nanoparticles significantly decreases after modification. The modified silica nanoparticles was dispersed in water using TX-100 as the dispersant and NaOH to adjust the pH. The dispersion was injected into an oil-treated artificial core, the injecting pressure of the NaCl solution (5 *wt* %) before and after injection was measured. The result showed that the hydrophobic silica nanoparticles exhibit a good pressure-decreasing ability. The contact angle of the slabbed core was measured, the contact angle increased from 36° to 134° after it was treated by the modified silica nanoparticle dispersion. Transmission electron microscopy was employed for the characterization of the modified silica nanoparticles. Scanning electron microscopy was employed for the characterization of the treated core; the result showed that the modified silica nanoparticles are adsorbed on the surface of the core and forms a hydrophobic layer, changing the wettability of the sand surface from water wet to oil wet, thereby decreasing the flowing pressure.

Keywords: silica nanoparticles; modification; dispersion; pressure-decreasing

1. Introduction

With the development of the global economy, the demand for oil is growing every year [1-2]. However, most conventional oilfields have been explored for several years, it is necessary to shift the focus to the development of unconventional oil resources, such as low-permeability oilfields [3-4]. Fracturing is necessary for exploring low-permeability oilfields [5]. After that, water flooding is conducted to displace the oil out. However, because of the existence of small pores and throats, as well as clay, in the formation rock, the water injecting pressure continuously increases when water flooding is conducted [6-8]. This will increase the cost of equipment and operation, as well as the security of production. Accordingly, decreasing the water injecting pressure is key for the development of low-permeability oilfields.

For decreasing pressure in oil production, acidizing [9], wettability reversal by surfactants [10], and molecular films [11] are three commonly used methods. Acidizing is a useful method for removing the plug and broadening the water flowing channel. However, the operation is expensive and needs to be repeated to maintain the effect. The surfactant can be adsorbed on the rock surface, thereby changing the surface from hydrophilic to hydrophobic and decreasing the water injecting pressure. Nevertheless, the surfactant may emulsify the residual oil, and the emulsion formed may block the rock channel and throat. On the other hand, molecular films represent a new method for decreasing the water injecting pressure, and the mechanism is similar to that of a surfactant. While the adsorption of molecules is mainly dependent on

molecular forces and hydrogen bonds, the effective time is always short.

The excellent physical and chemical properties of nanomaterials provide some new ideas for solving the above mentioned issue [12-16]. Various methods have been developed for preparing nanoparticles and for evaluating their properties [17-19]. However, because these nanoparticles exhibit high surface energy, they tend to aggregate in the medium and exhibit poor dispersion capacity in oil and organic solvents, thus, the applications of several nanoparticles are significantly limited. Fortunately, this problem can be resolved by some special preparation techniques, e.g., the surface modification of nanoparticles using some organic compounds [20-21]. As the surface modification agents are lyophilic, such as methyl, the modified nanoparticles can be stably dispersed in oil and organic solvents. ZnO, TiO_2, and PbS nanoparticles have been reported to be successfully modified with organic compounds with the aim of improving their dispersive capacity in oil and organic solvents [22-24].

Silica nanoparticles are the most productive and widely used among all nanoparticles [25-27]. Because of their special optical performance, light catalysis characteristics, and rheological properties, they have been widely applied in rubber, cement, paper, ceramics, medicine, and paint [28-30]. However, because of the existence of surface hydroxyl groups, silica nanoparticles are always hydrophilic. The high surface energy of silica nanoparticles also makes them tend to aggregate in the medium [31-32]. Surface modification is necessary for extending their application. Typically, silane coupling agents, halogenated silanes, polymers, and long-chain

aliphatic alcohols are the organic compounds used for the surface modification of silica nanoparticles. Monde *et al.* have modified the surface of the silica nanoparticles using enzyme molecules and biomembrane probes, the modified silica nanoparticles demonstrate potential for applications in biochemical analysis and biotechnology [33]. Navid *et al.* have prepared highly charged polyelectrolyte-grafted silica nanoparticles with sulfonated polystyrene sulfonate, and the modified silica nanoparticles were used for preparing stable trichloroethylene in water and heptane in water Pickering emulsions [34]. Sun *et al.* have added partially hydrophobic modified silica nanoparticles for enhancing the stability of nitrogen foam, the enhanced nitrogen foam was used for improving oil recovery, and the result showed that the enhanced nitrogen foam exhibits oil recovery higher than that exhibited by ordinary nitrogen foam [35]. However, none of these modified silica nanoparticles were utilized in pressure-decreasing applications for oil production.

***In situ* modification based on the sol–gel method [36] using siloxanes such as diethoxydimethylsilane or triethoxymethylsilane is an important method for synthesizing hydrophobic silica nanoparticles. However, the hydrolysis reaction is sensitive to pH. Furthermore, it is difficult to synthesize silica nanoparticles less than 100 nm. Moreover, it is difficult to control the size of the silica nanoparticles when the silica gel is heated. Compared with in situ modification, wet modification utilizes hydrophilic silica nanoparticles as raw materials. It is easy to control the size of the modified hydrophobic silica nanoparticles, besides, the modified reaction can be easily conducted.**

In this paper, dimethyldichlorosilane (DMCS) was used for the surface modification of silica nanoparticles. The modified silica nanoparticles were successfully dispersed in water and used to decrease the water injecting pressure. The pressure-decreasing mechanism of the modified silica nanoparticles was investigated and discussed. The results obtained herein can provide theoretical support for pressure-decreasing applications in oil production, especially low-permeability oilfields.

2. Materials and methods

2.1 Materials

Silica nanoparticles (15 nm) were purchased from Aladdin Reagent Company. The specific surface area of the sample was 359 nm^2/g. DMCS, NaOH, HCl, and NaCl were purchased from Sinopharm Chemical Reagent Co., Ltd. The commercial pressure-decreasing agent, hydrophobic silica nanoparticles MGS-W, and dispersant MGS-J were purchased from Zhengzhou Dongshen Chemical Technology Co., Ltd. The artificial core was purchased from Haian Oil Scientific Research Apparatus Co., Ltd with permeability ranging from 1×10^{-3} μm^2 to 50×10^{-3} μm^2. The mixture of dehydrated crude and kerosene with a viscosity of 3 mPa·s was used as the oil.

2.2 Apparatus and procedures

2.2.1 Modification and dispersion of silica nanoparticles

First, approximately 5 g of silica nanoparticles was added into a three-necked flask, second, silica nanoparticles were heated to 120 ℃ and stirring was maintained for 2 h for removing the moisture. Third, 95 g of anhydrous ethanol was added for dispersing

silica nanoparticles. Fourth, the stirring of the mixture was maintained for another 10 min, followed by the addition of 1 g of DMCS and 0.3 g of distilled water. Next, after reacting for 2 h at 90 °C, the suspension was filtered under vacuum and washed 4–6 times using anhydrous ethanol until all residues were removed. Finally, the filter cake was dried in a vacuum drying box for 24 h at 120 °C and ground to obtain modified silica nanoparticles.

The modified silica nanoparticles thus obtained were dispersed as follows. First, 1000 mL of distilled water was added into a beaker, followed by the addition of 4.5 g of TX-100. Second, the solution was stirred for approximately 10 min in a water bath at 25 °C. Third, 1.8 g of modified silica nanoparticles was slowly added into the solution. Next, 1 mol/L of NaOH was added dropwise when the temperature of the water bath was increased to 80 °C until the dispersion became clear and transparent. The zeta potential of the dispersion was measured using a Malvern Zetasizer Nano ZS90 instrument.

MGS-W was dispersed in water along with MGS-J as the dispersant in the same method. The amount of TX-100 and modified silica nanoparticles can be adjusted according to the requirement.

2.2.2 Core flowing experiment

First, the artificial core was dried in an oven at 100 °C for 24 h for removing the moisture. Second, the dry weight W_1 of the core and the diameter d and length L of the core were measured. Third, the core was dipped into a 5% NaCl solution and subjected to vacuum for 24 h for saturating it with saline. Then, the wet weight W_2

was measured. The saturated core was placed into a core holder, and a surrounding pressure of 2.0 MPa was applied. Then, a 5% NaCl solution was injected into the core at a constant rate *(Q)* of 1 mL/min, and the injecting pressure *P* was measured. After that, the water was displaced out with oil at a rate of 0.1 mL/min for saturating the core with oil. The core was aged for three days and displaced using a NaCl solution at a rate of 1 mL/min until no oil flowed out. The displacement pressure P_1 was measured. Approximately 1 pore volume *(PV)* modified silica nanoparticles dispersion was injected into the oil-treated core at a rate of 1 mL/min. The core was aged for another 24 h to allow for the adequate adsorption of modified silica nanoparticles on the sand surface. The following NaCl solution (5 wt%) was injected, and the injecting pressure P_2 was measured. The dispersion of the modified silica nanoparticles was replaced by WGS-W dispersion and TX-100 solution, and the experiment was repeated in the same process. Fig. 1 shows the diagram of the experimental instrument.

2.2.3 Characterization of modified silica nanoparticles

A NEXUS reflectance infrared spectrometer (American Thermo Nicolet Company) was used to characterize silica nanoparticles by the KBr disk method.

The titration method was employed for quantitatively determining the surface hydroxyl number, as described by Pan et al. [37]. First, approximately 2 g of silica nanoparticles was added to a 200 mL beaker, followed by the addition of 20% of a 75 g NaCl solution and 25 mL of anhydrous ethanol. Second, the pH of the mixture was adjusted to 4 using a 0.1 mol/L of an HCl or NaOH solution. Third, the pH of the

mixture was titrated to 9 by using a 0.1 mol/L NaOH solution and maintained for 20 s. The surface hydroxyl number of sample can be calculated using formula 1:

$$N = \frac{CVN_A \times 10^3}{Sm} \quad (1)$$

C is the NaOH concentration (0.1 mol/L), V is the NaOH volume (mL) consumed when the pH increased from 4 to 9, N_A is the Avogadro's number, S is the specific surface area of the sample (nm^2/g), and m is the quality of silica nanoparticles (g).

X-ray photoelectron spectroscopy (XPS) spectrum of raw silica nanoparticles and modified silica nanoparticles were recorded using an XPS multi-functional surface measurement and analysis system ESCALAB250 (American Thermo-VG Scientific). Survey (0–1000 eV) and high-resolution spectra (C1s) were recorded at a pass energy of 150 eV. XPS test instrument conditions were as follows: target voltage and target current of the Al K_α excitation source were 15 kV and 10 mA, respectively. The vacuum chamber pressure was less than 2×10^{-6} Pa, the measurement step length was 0.1 eV, the sputtering speed was 0.2 nm/s, and the sputtering area was 2 mm × 2 mm. The required XPS standard spectral data were obtained from the XPS manual.

Thermogravimetric analysis (TGA) was conducted on an SDT Q600 Simultaneous DSC-TGA (TA Instruments) for determining the amount of $–CH_3$ that has been grafted on the surface of the silica nanoparticles. Both raw silica nanoparticles and modified silica nanoparticles were tested. The linear heating rate was always 10 °C/min, and the samples were heated under nitrogen at a flow rate of 50 mL/min.

Transmission electron microscopy (TEM, Japanese electronics JEM-2100) was used to characterize the modified silica nanoparticles.

Field-emission scanning electron microscopy (FE-SEM) was employed for the characterization of the adsorption of modified silica nanoparticles on the core surface.

The contact angle of the core cutter treated by modified silica nanoparticles was measured using a HARKE-SPCA contact angle measuring instrument from the Beijing Hakko test instrument factory. The surface of the slabbed core was dipped into the modified silica nanoparticles for 24 h after it was planished, and then the slabbed core was dried in the oven. Next, the circular drop method was employed for measuring the contact angle of water for the core cutter.

3. Results and Discussion

3.1 Characterization of modified silica nanoparticles

FTIR was employed for the characterization of silica nanoparticles. As shown in Fig. 2, both samples exhibited a very strong absorption peak at 1000–1100 cm^{-1}, attributed to the stretching vibration of the Si–O–Si bond. A strong absorption peak was also observed at 1630 cm^{-1}, attributed to the bending vibration of H–O–H of water. Furthermore, another absorption peak was observed at 3400 cm^{-1}, attributed to the stretching vibrations of the hydroxyl group, this result confirms the existence of hydroxyl groups on the silica surface. The new absorption peak at around 3000 cm^{-1} was attributed to the methyl stretching vibration, and the intensity of the absorption peak at 3400 cm^{-1}, attributed to the hydroxyl groups, significantly decreased. This result is indicative of the decline of the surface hydroxyl number. The appearance of

the new absorption peak for methyl and weakening of the hydroxyl stretching vibration both confirm the successful grafting of methyl on the surface of silica nanoparticles.

The titration method was employed for quantitatively determining the surface hydroxyl number of silica nanoparticles. Approximately 15 mL and 2.8 mL of a NaOH solution were consumed during titration by silica nanoparticles and modified silica nanoparticles, respectively. As calculated from formula 1, the surface hydroxyl number of silica and modified silica nanoparticles was 1.28 nm^{-2} and 0.24 nm^{-2}, respectively. The surface hydroxyl number of silica nanoparticles decreased significantly after modification. As shown in Fig. 3, DMCS hydrolyzes in solution, and the highly reactive hydroxyl groups formed can react with the hydroxyl groups on the surface of silica nanoparticles, thereby decreasing the surface hydroxyl number.

XPS was an important method for determining the surface composition. Fig. 4a shows the XPS spectra of raw silica and modified silica nanoparticles: except for the peaks observed at 103.5 eV (Si–O) and 150.5 eV (Si 2s), attributed to Si, and that at 532.5 eV is attributed to O. The small peak of raw silica at 285.4 eV can be explained as the impurity in the sample. After modification, the peak at 285.4 eV (C-OR) enhanced significantly. In the C1s spectrum of the modified silica nanoparticles (Fig. 4b), the C element existed in the form of $-CH_3$, which confirms the modification of silica nanoparticles by DMCS.

TGA was employed for determining the amount of $–CH_3$ grafted on the surface of the silica nanoparticles. As shown in Fig. 5, for the raw silica

nanoparticles, when the temperature was increased from 25 °C to 120 °C, the sample weight decreased from 100% to 99%, attributed to the loss of adsorption water. After that, the weight decreased from 99% to 95% when the temperature was increased from 120 °C to 500 °C. This weight loss is attributed to the loss of condensation water from the polycondensation of surface hydroxyl groups. For the modified samples, when the temperature was increased from 25 °C to 550 °C, the sample weight decreased gradually from 100% to 96%, is also attributed to the loss of adsorption water and the loss of condensation water. On the other hand, when the temperature was increased from 550 °C to 800 °C, the weight decreased from 96% to 92.2%. This can be explained as the loss of methyl group grafted on the silica surface. The result proves that approximately 3.8% of -CH_3 is grafted on the surface of the silica nanoparticles.

3.2 Dispersion of modified silica nanoparticles

Fig. 6 shows the TEM image of the modified silica nanoparticles, the radius of the evenly distributed modified silica nanoparticles was approximately 15–20 nm. Because the methyl groups were grafted on the surface of the silica nanoparticles, the hydrophobicity of silica nanoparticles was significantly enhanced. As shown in Fig. 7a, the modified silica nanoparticles can be easily dispersed in organic solvents such as diesel. However, if the modified silica nanoparticles are to be widely applied in oilfields, large amounts of diesel will be consumed. Besides, the transportation and storage of diesel pose several security risks, and it increases the cost of operation as well, hence, it is necessary to replace diesel with other mediums such as water.

In this study, modified silica nanoparticles were successfully dispersed in water with TX-100 as the dispersant and NaOH to adjust the pH. As shown in Fig. 7b, it is difficult to disperse the silica nanoparticles in water because of their hydrophobic surface. Hence, a dispersant is necessary for dispersing the modified silica nanoparticles. The special amphipathic structure of the surfactant makes it an excellent candidate for a dispersant [38-39]. The surfactant tends to form aggregates such as spherical micelles, rod-like micelles, and vesicles, and the hydrophobic cavity of these aggregates can provide an ideal environment for modified silica nanoparticles [40-41]. When TX-100 is added into water, it dissolves in water and fully stretches, and the steric effect of TX-100 can prevent the particles from coalescence, thereby increasing the dynamic stability of the system. The zeta potential is also important for colloid systems [42]. When NaOH is introduced to the system, OH^- can be adsorbed on the surface of the modified silica nanoparticles, thereby increasing the charge amount and zeta potential of particles. Thus, the electrostatic repulsion between the modified silica nanoparticles was increased. Then, the coalescence stability of the system increased as well. The results of zeta potential measurement were found to be in agreement with the abovementioned results. The zeta potential increased from −12.3 mV to −27.5mV after NaOH was introduced. The stability of the system also significantly enhanced.

3.3 Core flowing experiment

Core parameters such as pore volume (PV), porosity (ϕ), and permeability (k) can be calculated as follows:

$$PV = \frac{w_2 - w_1}{\rho} \quad (2)$$

$$\varphi = \frac{4PV}{\pi d^2 L} \quad (3)$$

$$k = \frac{4Q\mu L}{\pi d^2 P} \quad (4)$$

ρ is the density of the NaCl solution, which is 1.034 g/cm^{-3}.

Table 1 shows the experimental results. As shown in Fig. 8, the pressure-decreasing percent of MGS-W pressure-decreasing agent was 32%, while that for the modified silica nanoparticle dispersion was 45%. The pressure-decreasing ability of the modified silica nanoparticle dispersion was significantly better than those of the TX-100 solution and MGS-W pressure-decreasing agent.

Table 1 Result of the core parameters and experiment

Core number	Treat solution	PV/mL	ϕ/%	k/×10^{-3} μm^2	P_1/MPa	P_2/MPa	Pressure decreasing percent/%
1	Modified SiO_2 dispersion	10.23	21.70	33	1.33	0.73	45.1
2	MGS-W dispersion	10.97	22.83	35	1.28	0.87	32.0
3	TX-100 solution	10.34	20.73	31	1.26	0.99	21.4

3.4 Pressure-decreasing mechanism discussion

The SEM images of the core before and after the treatment by the modified silica nanoparticles were recorded for investigating the interaction between the core and the modified silica nanoparticles. As shown in Fig. 9a, before the injection of modified silica nanoparticle dispersion, the surface of sandstone was smooth, with the exposed diagenetic mineral. After the modified silica nanoparticle dispersion was injected, the

salt made the dispersion unstable, thereby releasing the modified silica nanoparticles. As shown in Fig. 9b, the modified silica nanoparticles were adsorbed on the exposed sand surface, forming a hydrophobic layer on the sand surface.

The contact angle of water to the slabbed core was measured. As shown in Fig. 10a, the contact angle of water to the core was 36°, confirming the formation of a water-wet core. After the treatment of modified silica nanoparticles, as shown in Fig. 10b, the contact angle of water increased to 134°. That is, the sand surface changes from water wet to oil after the treatment.

The injecting well is always transformed from the production well when the production fluid is all water. Because of the long time washing and immersion of formation and injecting water, the formation rock surface changed from hydrophobic to hydrophilic. As shown in Fig. 11, a hydration shell was always formed on the rock surface when water flooding was conducted, and the injected water combined with the hydration shell, resulting in the increase in flow resistance and injection pressure. When the modified silica nanoparticle dispersion was injected into the core, the released modified silica nanoparticles formed a hydrophobic film on the sand surface, thereby crowding out the water on the sand surface and increasing the water flowing width. The modified silica nanoparticles can also move to the interlayers of clay minerals, discharge the interlayer water, and shrink the clay, which can also increase the water flowing channel.

Because the wettability of the rock changed from water wet to oil wet caused by the adsorption of modified silica nanoparticles, the contact angle of water to the sand

surface increases. The adhesion work equation is expressed as follows:

$$W = \sigma(1 + cos\ \theta) \quad (5)$$

σ is the interface tension between the rock and water, θ is the contact angle of water to the sand surface, and W is the adhesion work.

The adhesion work is mainly determined by interface tension and contact angle in a certain rock throat. If the sand surface was water wet, $\theta < 90°$, $\cos\theta > 0$, W was positive. This implies difficulty for the water to be displaced out by adhesion work. When the sand surface became oil wet, $\theta > 90°$, and $\cos\theta < 0$, W decreased. Now, it is easier to displace the water out. Thus, the water flowing resistance decreases, and the water injecting pressure accordingly decreases.

4. Conclusion

In summary, silica nanoparticles were modified with DMCS to change them from hydrophilic to hydrophobic. The modified silica nanoparticles were dispersed in water and first utilized to decrease the water injecting pressure for oil production. The result obtained from the core flowing experiment shows that the modified silica nanoparticles dispersion has good pressure-decreasing ability. Results obtained from SEM image and contact angle measurements demonstrate that modified silica nanoparticles can be adsorbed on the surface of exposed sand, which changes the rock surface from hydrophilic to hydrophobic and decreases the water flow resistance significantly. This will have broad applications in the development of oilfields to decrease the water-injecting pressure.

Acknowledgement

The study was supported by the National Key Basic Research Program of China (No.2015CB250904), National Science Fund for Distinguished Young Scholars (No.51425406), and Chang Jiang Scholars Program (No. T2014152).

References

[1] C. J. Campbell and J. H. Laherrère, The end of cheap oil. Scientific American, 1998, 3, 78-83.

[2] M. Asif and T. Muneer, Energy supply, its demand and security issues for developed and emerging economies, Renewable and Sustainable Energy Reviews, 2007, 11, 1388-1413.

[3] M. J. Small, P. C. Stern, E. Bomberg, S. M. Christopherson, B. D. Goldstein, A. L. Israel, R. B. Jackson, A. Krupnick, M. S. Mauter, J. Nash, D. W. North, S. M. Olmstead, A. Prakash, B. Rabe, A. Richardson, S. Tierney, T. Webler, G.Wong-Parodi and B. Zielinska, Risks and risk governance in unconventional shale gas development, Environmental science & technology, 2014, 48, 8289-8297.

[4] G. D. Vassilellis, Roadmap to monetization of unconventional resources, Society of Petroleum Engineers (SPE), 2009, SPE paper 121968.

[5] J. B. Curtis, Fractured shale-gas systems, AAPG bulletin, 2002, 86, 1921-1938.

[6] K. W. Shanley, R. M. Cluff and W. Robinson, Factors controlling prolific gas production from low-permeability sandstone reservoirs: Implications for resource assessment, prospect development, and risk analysis, AAPG bulletin, 2004, 88, 1083-1121.

[7] M. M Sharma, S. Pang, K. E. Wennberg and L. N. Morgenthaler, Injectivity decline in water-injection wells: an offshore Gulf of Mexico case study, SPE Production & Facilities, 2000, 15, 6-13.

[8] G. Q. Tang and A. Firoozabadi, Effect of pressure gradient and initial water saturation on water injection in water-wet and mixed-wet fractured porous media, SPE reservoir evaluation & engineering, 2001, 4,516-524.

[9] T. P. Huang, A. D. Hill and R. S. Schechter, Reaction rate and fluid loss: The keys to wormhole initiation and propagation in carbonate acidizing, SPE Journal, 2000, 5, 287-292.

[10] Y. Wu, P. J. Shuler, M. Blanco, Y. C. Tang and W. A. Goddard, An experimental study of wetting behavior and surfactant EOR in carbonates with model compounds, SPE Journal, 2008, 13, 26-34.

[11] C. L. Feng, Y. J. Zhang, J. Jin, Y. L. Song, L. Y. Xie, G. R. Qu, L. Jiang and D. B. Zhu, Reversible wettability of photoresponsive fluorine-containing azobenzene polymer in Langmuir-Blodgett films, Langmuir, 2001, 17, 4593-4597.

[12] S. Rüttermann, C. Wandrey, W. H. Raab and R. Janda, Novel nano-particles as fillers for an experimental resin-based restorative material, Acta biomaterialia, 2008, 4, 1846-1853.

[13] M. C. Daniel and D. Astruc, Gold nanoparticles: assembly, supramolecular chemistry, quantum-size-related properties, and applications toward biology, catalysis, and nanotechnology, Chemical reviews, 2004, 104, 293-346.

[14] C. A. Mirkin, R. L. Letsinger, R. C. Mucic and J .J. Storhoff, A DNA-based method for rationally assembling nanoparticles into macroscopic materials, Nature, 1996, 382, 607-609.

[15] M. Brust, M. Walker, D. Bethell, D. J. Schiffrin and R. Whyman, Synthesis of

thiol-derivatised gold nanoparticles in a two-phase liquid–liquid system, J. Chem. Soc, Chem. Commun, 1994, 7, 801-802.

[16] S. Sun, C. B. Murray and D. Welle, Monodisperse FePt nanoparticles and ferromagnetic FePt nanocrystal superlattices, Science, 2000, 287, 1989-1992.

[17] R. Ledezma, M. Esther Trevino, L. E. Elizalde, L. A. Pérez-Carrillo, L. Mendizábal, J. E. Puig and R. G. López, Semicontinuous heterophase polymerization under monomer starved conditions to prepare nanoparticles with narrow size distribution, Journal of Polymer Science Part A: Polymer Chemistry, 2007, 45, 1463-1473.

[18] S. Nakade, M. Matsuda, S. Kambe, Y. Saito, T. Kitamura, T. Sakata, Y. Wada, H. Mori and S. Yanagida, Dependence of TiO_2 nanoparticle preparation methods and annealing temperature on the efficiency of dye-sensitized solar cells, The Journal of Physical Chemistry B, 2002, 106, 10004-10010.

[19] N. Sahiner, H. Ozay, O. Ozay and N. Aktas, A soft hydrogel reactor for cobalt nanoparticle preparation and use in the reduction of nitro phenols, Applied Catalysis B: Environmental, 2010, 101, 137-143.

[20] R. P. Bagwe, L. R. Hilliard and W. Tan, Surface modification of silica nanoparticles to reduce aggregation and nonspecific binding, Langmuir, 2006, 22, 4357-4362.

[21] I. J. Bruce and T. Sen, Surface modification of magnetic nanoparticles with alkoxysilanes and their application in magnetic bioseparations, Langmuir, 2005, 21, 7029-7035.

[22] R. Y. Hong, J. H. Li, L. L. Chen, D. Q. Liu, H. Z. Li, Y. Zheng and J. Ding, Synthesis, surface modification and photocatalytic property of ZnO nanoparticles, Powder Technology, 2009, 189, 426-432.

[23] X. Li, W. Chen, C. Bian, J. B. He, N. Xua and G. Xue, Surface modification of TiO_2 nanoparticles by polyaniline, Applied Surface Science, 2003, 217, 16-22.

[24] S. Chen, W. Liu and L. Yu, Preparation of DDP-coated PbS nanoparticles and investigation of the antiwear ability of the prepared nanoparticles as additive in liquid paraffin, Wear, 1998, 218, 153-158.

[25] M. Q. Zhang, M. Z. Rong, H. B. Zhang and K. Friedrich, Mechanical properties of low nano-silica filled high density polyethylene composites, Polymer Engineering & Science, 2003, 43, 490-500.

[26] H. Ow, D. R. Larson, M. Srivastava, A. B. Barbara, W. W. Watt and W. Ulrich, Bright and stable core-shell fluorescent silica nanoparticles, Nano letters, 2005, 5, 113-117.

[27] H. K. Xu, J. B. Quinn and A. A. Giuseppetti, Wear and mechanical properties of nano-silica-fused whisker composites, Journal of dental research, 2004, 83, 930-935.

[28] A. J. Kinloch, R. D. Mohammed, A. C. Taylor, C. Eger, S. Sprenger and D. Egan, The effect of silica nano particles and rubber particles on the toughness of multiphase thermosetting epoxy polymers, Journal of Materials Science, 2005, 40, 5083-5086.

[29] L. Senff, J. A. Labrincha, V. M. Ferreira, D. Hotzaa and W. L. Repette, Effect of

nano-silica on rheology and fresh properties of cement pastes and mortars, Construction and Building Materials, 2009, 23, 2487-2491.

[30] H. K. Xu, D. T. Smith and C. G. Simon, Strong and bioactive composites containing nano-silica-fused whiskers for bone repair, Biomaterials, 2004, 25, 4615-4626.

[31] Y. H. Lai, M. C. Kuo, J. C. Huang and M. Chen, On the PEEK composites reinforced by surface-modified nano-silica, Materials Science and Engineering: A, 2007, 458, 158-169.

[32] K. C. Park, H. J. Choi, C. H. Chang, R. B. Cohen, G. H. McKinley and G. Barbastathis, Nanotextured silica surfaces with robust superhydrophobicity and omnidirectional broadband supertransmissivity, Acs Nano, 2012, 6, 3789-3799.

[33] M. Qhobosheane, S. Santra, P. Zhang and W. H. Tan, Biochemically functionalized silica nanoparticles, Analyst, 2001, 126, 1274-1278.

[34] N. Saleh, T. Sarbu, K. Sirk, G. V. Lowry, K. Matyjaszewski and R. D. Tilton, Oil-in-water emulsions stabilized by highly charged polyelectrolyte-grafted silica nanoparticles, Langmuir, 2005, 21, 9873-9878.

[35] Q. Sun, Z. M. Li, S. Y. Li, L. Jiang, J. Q. Wang and P. Wang, Utilization of surfactant-stabilized foam for enhanced oil recovery by adding nanoparticles, Energy & Fuels, 2014, 28, 2384-2394.

[36] I. Yuko, K. Shinzo, In situ formed silica particles in rubber vulcanizate by the sol-gel method, Polymer, 1997, 38, 4417-4423.

[37] P. Mao, Titration method for the determination of fumed silica specific surface

area, Chemical world, 1993, 8, 380-383.

[38] S. Haas, H. W. Hässlin and C. Schlatter, Influence of polymeric surfactants on pesticidal suspension concentrates: dispersing ability, milling efficiency and stabilization power, Colloids and Surfaces A: Physicochemical and Engineering Aspects, 2001, 183, 785-793.

[39] J. Lv, L. Qiu and B. Qu, Controlled growth of three morphological structures of magnesium hydroxide nanoparticles by wet precipitation method, Journal of Crystal Growth, 2004, 267, 676-684.

[40] H. Okuzaki and Y. Osada, Ordered-aggregate formation by surfactant-charged gel interaction, Macromolecules, 1995, 28, 380-382.

[41] N. J. Turro, X. G. Lei, K. P. Ananthapadmanabhan and M. Aronson, Spectroscopic probe analysis of protein-surfactant interactions: the BSA/SDS system, Langmuir, 1995, 11, 2525-2533.

[42] J. M. Berg, A. Romoser, N. Banerjee, R. Zebda and C. M. Sayes, The relationship between pH and zeta potential of 30 nm metal oxide nanoparticle suspensions relevant to in vitro toxicological evaluations, Nanotoxicology, 2009, 3, 276-283

Figure Captions:

Fig. 1: Instrument diagram for the core flowing experiment.

Fig. 2: FTIR spectra of silica nanoparticles (black line) and modified silica nanoparticles (red line).

Fig. 3: Mechanism of the modification of silica nanoparticles by DMCS.

Fig. 4: XPS spectrum of silica nanoparticles and modified silica nanoparticles (a) and C1s XPS spectrum of modified silica nanoparticles (b).

Fig. 5: TGA curves of silica nanoparticles (black line) and modified silica nanoparticles (red line).

Fig. 6: TEM image of modified silica nanoparticles.

Fig. 7: Images of modified silica nanoparticles dissolved in diesel (a) and water (b).

Fig. 8: Pressure change for modified silica nanoparticle dispersion (1), MGS-W (2) and TX-100 solution (3).

Fig. 9: SEM images of sand surface before (a) and after (b) the adsorption of modified silica nanoparticles.

Fig. 10: Contact angle of water on slabbed core before (a) and after (b) the treatment of modified silica nanoparticle dispersion.

Fig. 11: Pressure-decreasing mechanism for modified silica nanoparticles.

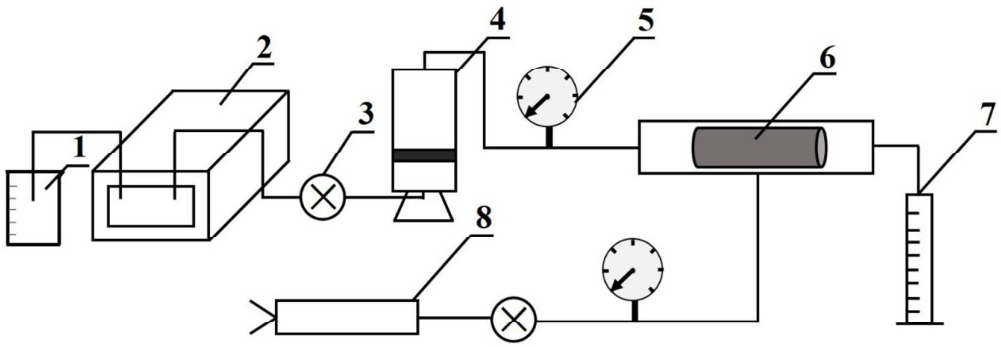

1. Distilled water 2. Pump 3. Valve 4. Container 5. Pressure gauge

6. Core holder 7. Cylinder 8. Hand pump

Fig. 1

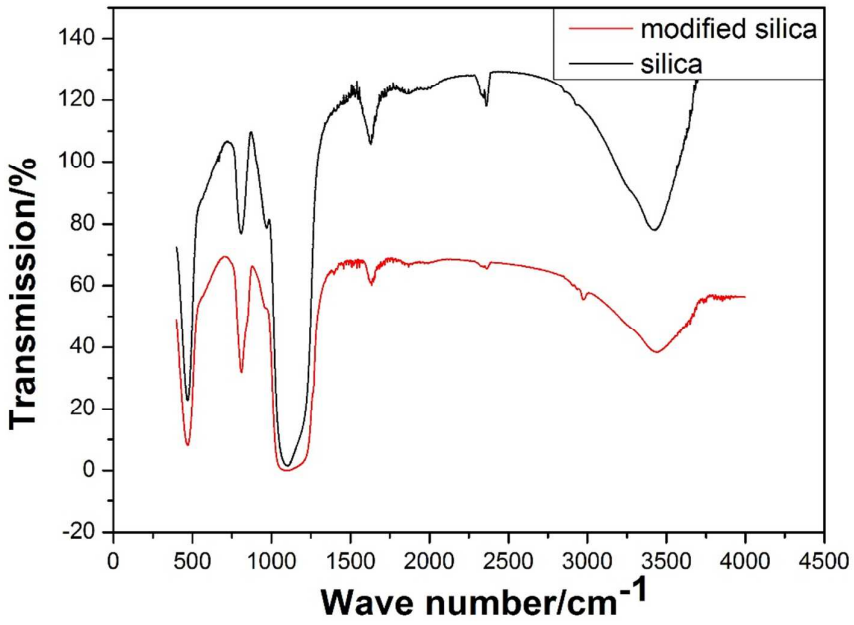

Fig. 2

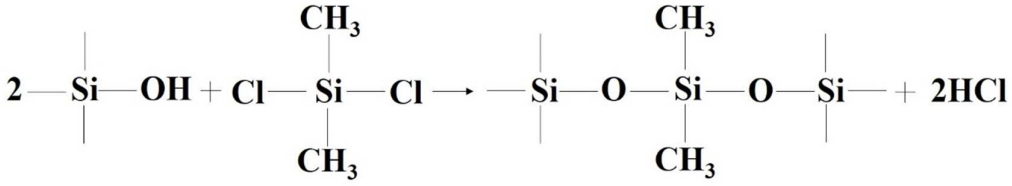

Fig. 3

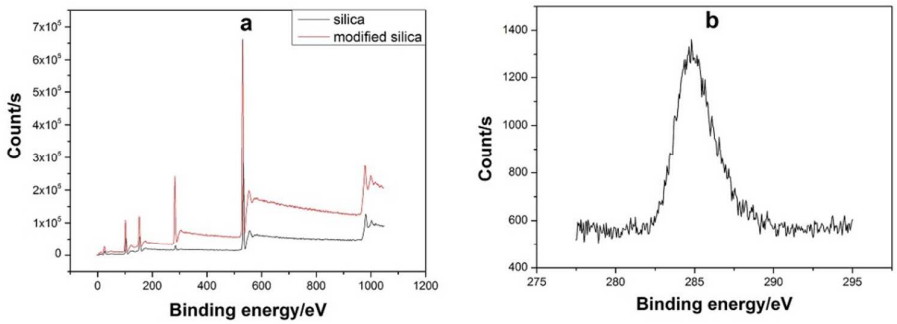

Fig. 4

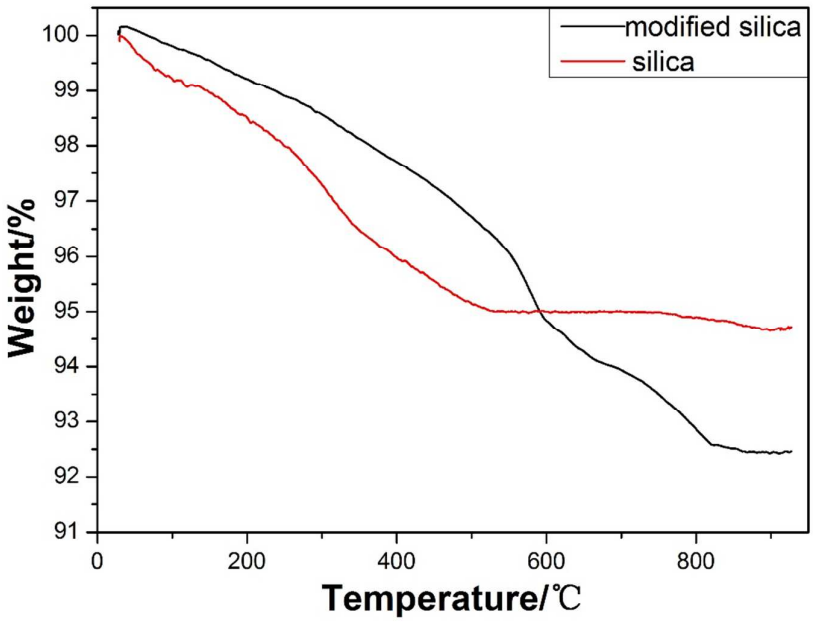

Fig. 5

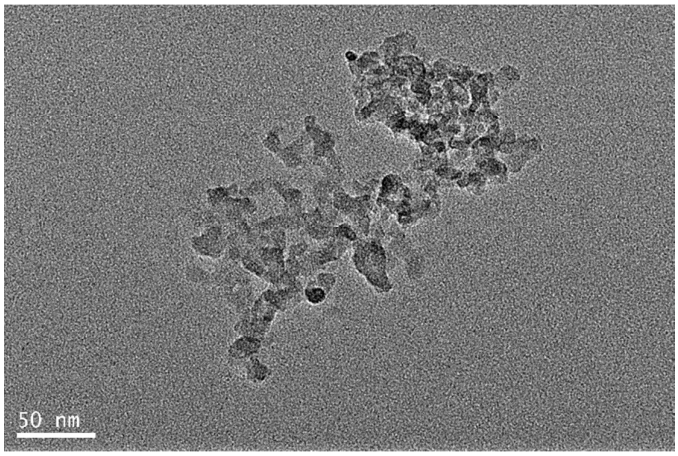

Fig. 6

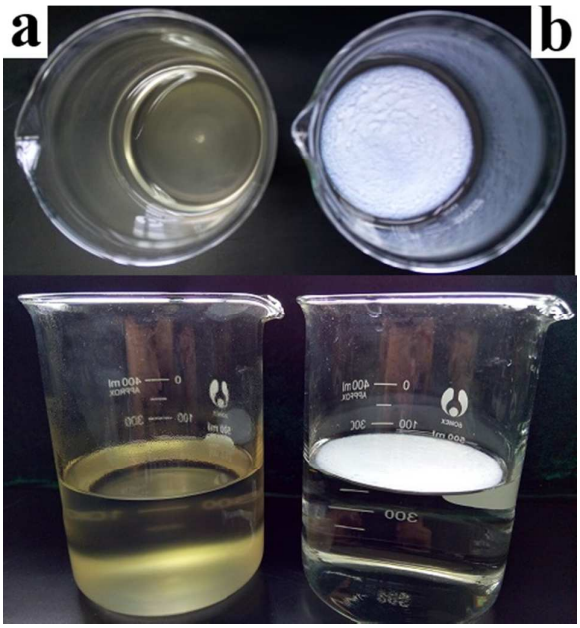

Fig. 7

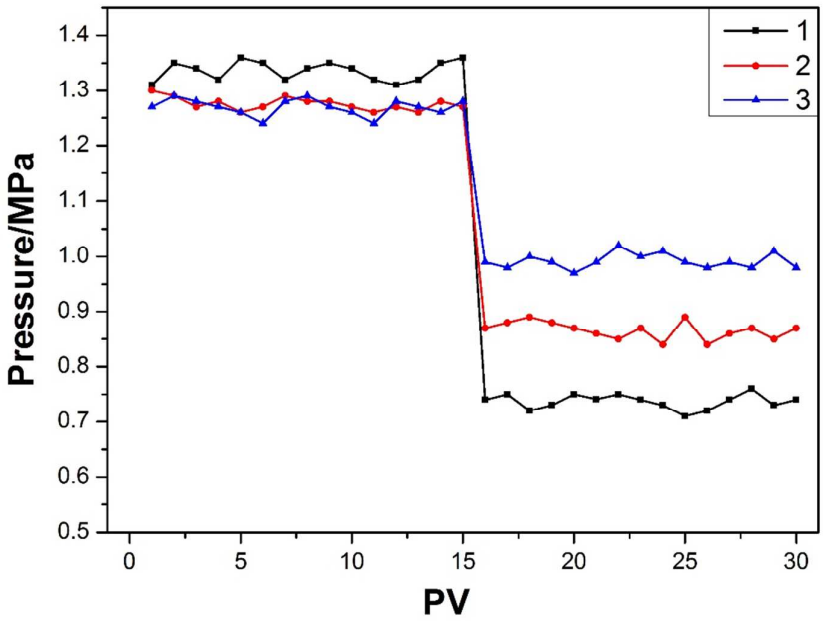

Fig. 8

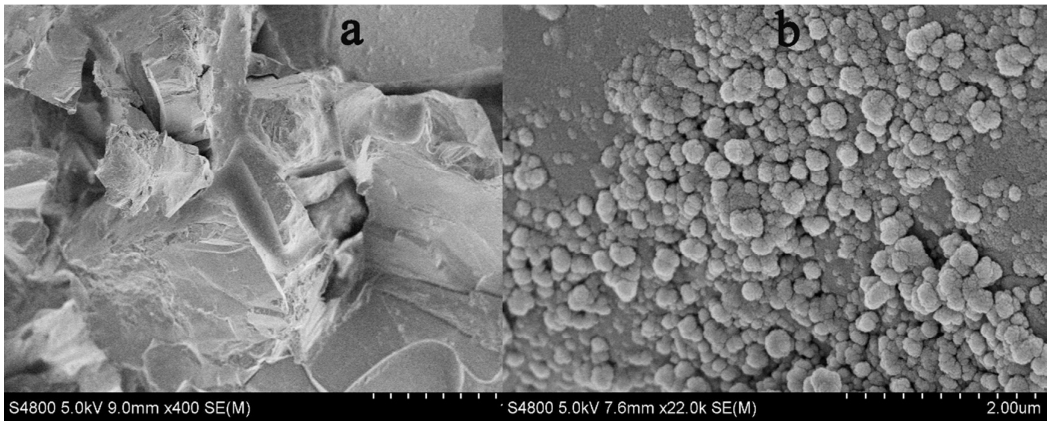

Fig. 9

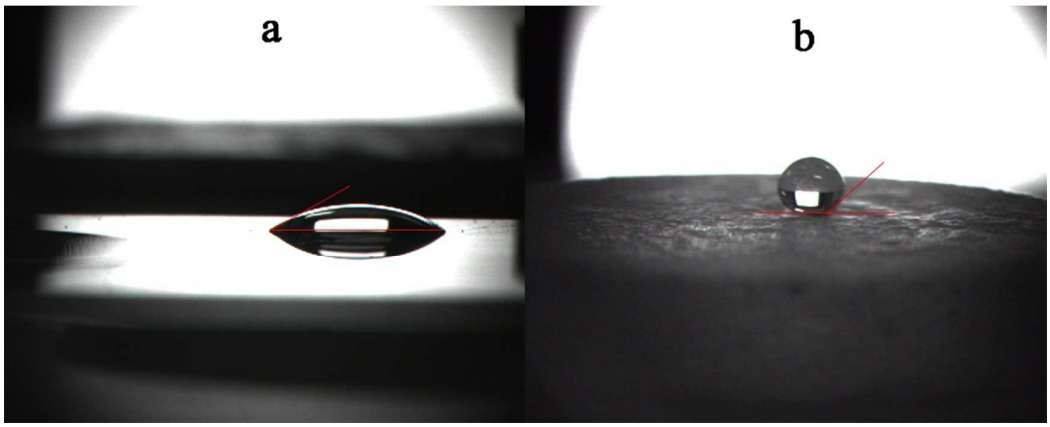

Fig. 10

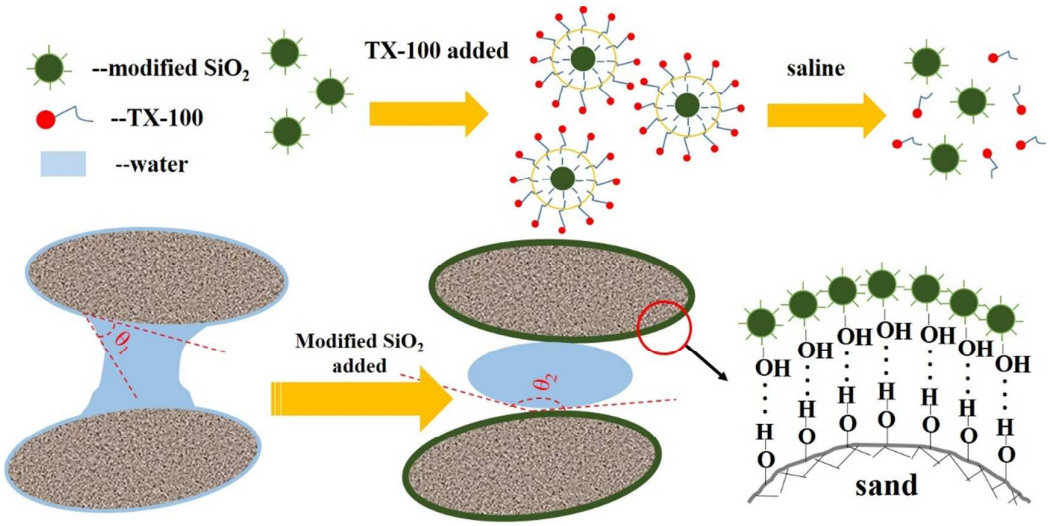

Fig. 11